Available online at www.sciencedirect.com
ScienceDirect
Developmental Biology 299 (2006) 257–271
DEVELOPMENTAL BIOLOGY
www.elsevier.com/locate/ydbio

Cellular electroporation induces dedifferentiation in intact newt limbs

Donald L. Atkinson [a,1], Tamara J. Stevenson [a,1], Eon Joo Park [b], Matthew D. Riedy [c], Brett Milash [d], Shannon J. Odelberg [a,b,c,*]

[a] Department of Internal Medicine, Division of Cardiology, University of Utah, Salt Lake City, UT 84132, USA
[b] Department of Neurobiology and Anatomy, University of Utah, Salt Lake City, UT 84132, USA
[c] Interdepartmental Program in Neuroscience, University of Utah, Salt Lake City, UT 84132, USA
[d] Huntsman Cancer Institute, University of Utah, Salt Lake City, UT 84132, USA

Received for publication 15 March 2006; revised 14 July 2006; accepted 25 July 2006
Available online 29 July 2006

Abstract

Newts have the remarkable ability to regenerate lost appendages including their forelimbs, hindlimbs, and tails. Following amputation of an appendage, the wound is rapidly closed by the migration of epithelial cells from the proximal epidermis. Internal cells just proximal to the amputation plane begin to dedifferentiate to form a pool of proliferating progenitor cells known as the regeneration blastema. We show that dedifferentiation of internal appendage cells can be initiated in the absence of amputation by applying an electric field sufficient to induce cellular electroporation, but not necrosis or apoptosis. The time course for dedifferentiation following electroporation is similar to that observed following amputation with evidence of dedifferentiation beginning at about 5 days postelectroporation and continuing for 2 to 3 weeks. Microarray analyses, real-time RT-PCR, and in situ hybridization show that changes in early gene expression are similar following amputation or electroporation. We conclude that the application of an electric field sufficient to induce transient electroporation of cell membranes induces a dedifferentiation response that is virtually indistinguishable from the response that occurs following amputation of newt appendages. This discovery allows dedifferentiation to be studied in the absence of wound healing and may aid in identifying genes required for cellular plasticity.

Keywords: Dedifferentiation; Cellular plasticity; Regeneration; Electric field; Electroporation; Newt; *Notophthalmus viridescens*

Introduction

Newts have the ability to regenerate lost appendages and injured organs, including their limbs, tails, spinal cords, retinas, lenses, optic nerves, jaws, heart ventricles, and intestines (Brockes and Kumar, 2002; Butler and Ward, 1967; O'Steen, 1958; Turner and Singer, 1974a,b). These regenerative events are dependent upon an unusual degree of cellular plasticity near the site of injury. For example, following limb or tail amputation, the wound is closed within 1 day by the migration of epithelial cells from the proximal epidermis. The internal cells underlying this newly formed wound epithelium begin to dedifferentiate to form a pool of proliferating progenitor cells known as the regeneration blastema. This dedifferentiation process is characterized in vivo by a general histolysis of the internal tissues, cell cycle reentry in normally quiescent cells, down-regulation of cell differentiation markers, and up-regulation of blastemal markers (Bodemer and Everett, 1959; Chalkley, 1954; Hay and Fischman, 1961; Kintner and Brockes, 1984; Thornton, 1938a,b). Later in the regenerative process, the blastemal cells will redifferentiate to form all of the internal tissues of the regenerated structure, except the nerve axons.

Loss of an appendage or injury of an organ initiates a regenerative response involving the dedifferentiation of cells near the wound. Several studies have suggested that severe injury is the main requirement for inducing regeneration or the related phenomenon of supernumerary limb formation. Supernumerary limbs can form when a deep incision is made through the limb followed by the placement of a tight ligature through the incision and around the remaining uncut portion of the limb (Della Valle, 1913; Tsonis, 1996; Wallace, 1981). Application of carcinogens or inflammatory substances to a urodele limb can induce dedifferentiation of internal tissues and supernumerary limb

* Corresponding author. University of Utah Health Sciences Center, Wintrobe Building, Room 667, 26 North 1900 East, Salt Lake City, UT 84132, USA. Fax: +1 801 581 8552.
E-mail address: odelberg@genetics.utah.edu (S.J. Odelberg).
[1] These authors contributed equally to this work.

0012-1606/$ - see front matter © 2006 Elsevier Inc. All rights reserved.
doi:10.1016/j.ydbio.2006.07.027

formation (Breedis, 1952; Tsonis and Eguchi, 1981). Crushing injuries can also produce a regenerative response that perfectly repairs the tissues of the crushed region (Mescher, 1982).

We show here that application of an electric field sufficient to cause electroporation of internal limb cells, but insufficient to cause necrosis or apoptosis, can initiate a dedifferentiation process characterized by cell cycle reentry of appendage cells, histolysis of internal tissues, and appropriate regulation of differentiation and blastemal markers. There is a direct correlation between pore formation in cell membranes and dedifferentiation of internal limb cells, suggesting that widespread, quickly reversible cell membrane damage is sufficient to initiate the dedifferentiation process. Microarray and real-time RT-PCR analyses reveal that electroporated and amputated newt limbs exhibit similar temporal gene expression patterns, whereas in situ hybridization experiments suggest that up-regulated genes are expressed in the same tissues following both types of injuries. These results indicate that at the histological, cellular, and molecular levels, amputation- and electroporation-induced dedifferentiation are virtually indistinguishable. This discovery allows dedifferentiation to be studied in the absence of the wound healing process that normally follows appendage amputation and may aid researchers in identifying genes required for the cellular plasticity response.

Materials and methods

Care of animals

Adult newts, *Notophthalmus viridescens*, were obtained from Charles Sullivan and housed in large tanks containing slow-flowing dechlorinated water. Newts were fed live California blackworms. All animal protocols were approved by the University of Utah Institutional Animal Care and Use Committee.

Amputations and collection of regenerating tissues

Newts were anesthetized by submersion in Tris-buffered 0.1% tricaine (pH 7.3) for 10 min and then placed on ice. Limb amputations were performed through the stylopodium of the forelimb or hindlimb midway between the proximal and distal epiphyses of the humerus or femur. The bone was not trimmed following amputation. Tail amputations were performed 1 cm from the distal tip of the tail. Newts were allowed to recover on ice for 1 h and then placed in shallow water with their heads above the surface until they recovered from anesthesia. Once conscious, the newts were housed in dechlorinated water until the regenerating tissues were collected for analyses.

Newts that were to be used to assess cell cycle reentry and histolysis were injected intraperitoneally with 0.1 ml of 10 mM BrdU 12 h before sacrifice. Forelimb tissues were collected for this analysis at 1, 2, 3, 4, 5, 6, 7, 14, 21, 28, and 35 days postamputation. Hindlimb and tail tissues were collected at 14 days postamputation. Newts that were to be used for immunofluorescence or apoptosis assays were not injected with BrdU. To collect the regenerating tissues, the newts were anesthetized as described above and the limbs were reamputated at either the shoulder or hip. Tails were reamputated 1 cm proximal to the regenerating tip. The regenerating tissues from BrdU-injected newts were fixed overnight in Carnoy's fixative (60% ethanol, 30% chloroform, 10% glacial acetic acid), whereas those tissues that were to be used for apoptosis assays were fixed in 4% paraformaldehyde in PBS overnight. Tissues fixed in Carnoy's were then decalcified for 1 h in 2 M HCl/PBS/0.5% Triton X-100, rinsed twice in PBS, dehydrated through a series of ethanol/PBS washes with increasing concentration of ethanol, treated with Hemo-De, and embedded in paraffin blocks. Tissues fixed in paraformaldehyde were embedded in paraffin blocks using the same procedure, except that the decalcification step was omitted. Tissues to be used for immunofluorescence assays were fixed in a paraformaldehyde–lysine-periodate fixative (0.05% paraformaldehyde, 100 mM lysine–HCl, 10 mM sodium periodate, 120 mM NaCl, 3 mM KCl, 10 μM $CaCl_2$, 5 mM HEPES, pH 7.4) for 45 min, rinsed in wash solution (120 mM NaCl, 3 mM KCl, 10 μM $CaCl_2$, 5 mM HEPES, pH 7.4) for 30 min, and frozen in O.C.T. for cryosectioning.

Application of electric fields to newt limbs and tails

Newts were anesthetized as described above and then gently strapped to an IC-Spacing perfboard (RadioShack) with Stretch Magic elastic cord (Helby Import Co.) to prevent movement of the limbs or tail during the application of the electric field. The newts were submerged in PBS and 3 mm Genetrodes (BTX) were placed parallel to the proximal–distal axis, one on the anterior side of the stylopodium and the other on the posterior side (Fig. 1). For tails, the electrodes straddled the tail and ran parallel to its proximal–distal axis. The gap between the electrodes was 3 mm for newt forelimbs and tails and 4 mm for newt hindlimbs. This allowed the electrodes to be placed such that they were not contacting the newt skin on either side of the limb or tail. Electric fields ranging from 33 to 167 V/cm were applied in five 100-ms pulses with 1 s between each pulse. Pilot studies had indicated that this was an effective range of electric field strengths for producing cellular electroporation, while not overtly damaging the limb tissue. Following the application of the electric field, the newts were placed on ice for 10 min and then allowed to recover from anesthesia as described above.

For ectopic *EGFP* expression, 3 μg of the expression construct pCMV-SPORT6-EGFP was injected in a 1-μl volume into the dorsal muscles of the stylopodium using a Drummond II Nanoject injector and a glass needle with a bore size of at least 60 μm. Electroporation was accomplished by pulsing using electric fields ranging from 33 to 167 V/cm electric field as described above. Limbs were monitored for *EGFP* expression over several weeks using a Zeiss M^2Bio fluorescence Stemi SV 11 stereomicroscope and photographs were taken using a MicroMax cooled, high-performance digital camera (Princeton Instruments).

Collection of electroporated limbs and tails

Newts were injected with BrdU as described above when the collected tissues were to be used for assessing cell cycle reentry or histolysis. Time points for the collection of electroporated tissues were the same as those used for amputated tissues (see above). Limbs and tails were collected and either embedded in paraffin after fixing the tissues overnight in Carnoy's fixative or 4% paraformaldehyde in PBS or embedded in O.C.T. after briefly fixing in the paraformaldehyde–lysine–periodate solution as described above.

Cell cycle reentry and histolysis assays

Decalcified tissues were sectioned at 10 μm and the paraffin was removed by washing the slides twice in Hemo-De for 10 min. The tissues were rehydrated in a series of solutions containing increasing amounts of PBS-0.5% Triton X-100 (PBSTx) and decreasing amounts of ethanol. Tissues were treated with 2 M HCl–PBSTx for 1 h to denature the DNA and then neutralized for 1 min in 100 mM sodium borate (pH 8.4). Following two rinses in PBS, endogenous peroxidases were inactivated by incubating the tissues in 1% hydrogen peroxide for 30 min and immunohistochemistry was performed according to the manufacturer's instructions using anti-BrdU as the primary antibody (Chemicon; 1/350 dilution in PBS) and the Elite Mouse IgG Vectastain ABC Kit (Vector Laboratories). Tissues were incubated with the DAB substrate for 10 min, rinsed for 5 min in tap water, and counterstained for 10 s with a 1/3 dilution of Gill #3 hematoxylin. The tissues were rinsed for 5 min in running tap water, dipped 10 times in acid rinse solution (4 ml glacial acetic acid in 196 ml ddH_2O), dipped 10 times in tap water, and incubated in bluing solution (3 ml NH_4OH in 197 ml of 70% ethanol). The slides were dipped 10 times in tap water and then dehydrated through a series of solutions containing increasing amounts of ethanol. The tissues were placed in Hemo-De and mounted with Cytoseal.

Immunofluorescence assays

Frozen tissues were cryosectioned at 10 μm and immunofluorescence assays were performed as described by Kintner and Brockes (1984) using the

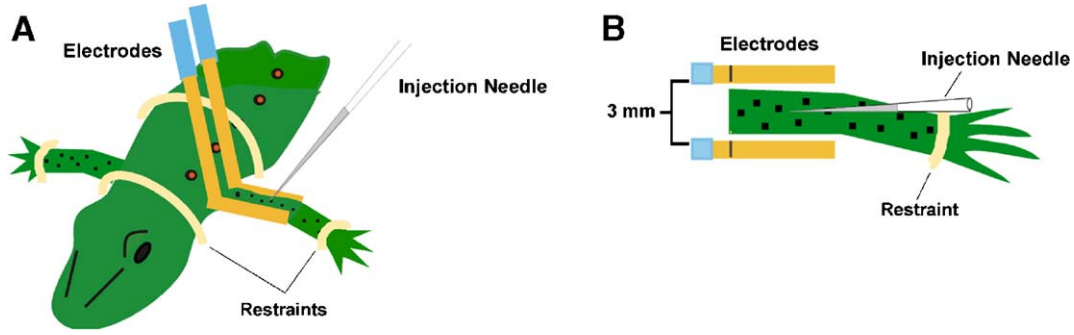

Fig. 1. Method used to apply electric fields to newt forelimbs. (A) Anesthetized newts were gently strapped to an IC-Spacing perfboard with Stretch Magic elastic cord (restraints). Restraints were applied to the neck, trunk, and both forelimbs. Newts were submerged in PBS and electrodes were placed parallel to the stylopodium so that the electrodes did not touch the skin. (B) An enlarged dorsal view of panel A showing that the electrodes were spaced 3 mm apart to prevent contact with the skin. The electric field was applied in pulses as described in the Materials and methods section. For EGFP expression, the expression construct was injected as shown just prior to applying the electric field. Injections were not performed in experiments designed to determine the effect of electric fields on intact limbs.

anti-12/101 (Kintner and Brockes, 1984) and anti-MT1 (Onda et al., 1991) mouse monoclonal antibodies (antibodies were obtained from the Developmental Studies Hybridoma Bank at the University of Iowa). The primary anti-12/101 (IgG) and anti-MT1 (IgM) antibodies were diluted 1/100 and 1/50, respectively, in 100 mM phosphate buffer (81 mM Na_2HPO_4+19 mM NaH_2PO_4) and a secondary Alexa 594-conjugated goat anti-mouse IgG or goat anti-mouse IgM antibody (Molecular Probes) was diluted 1/200. Primary antibodies were allowed to react with tissue sections for 45 min at room temperature and the secondary antibodies were incubated with the tissues for 30 or 45 min. The slides were mounted using the Slow Fade Light Anti-fade Kit with DAPI according to manufacturer's instructions (Molecular Probes).

TUNEL assay for apoptosis and histological examination for necrosis

Paraformaldehyde-fixed and paraffin-embedded tissues were sectioned at 10 μm, deparaffinized by Hemo-De, and gradually rehydrated in PBS. Given that these tissues were not decalcified, only regions containing soft tissues (e.g., epidermis, dermis, and muscle) were sectioned. TUNEL assays were performed according to manufacturer's instructions using the In Situ Cell Death Detection Kit, POD (Roche). Briefly, tissue sections were incubated in 3% H_2O_2 in methanol for 10 min to inactivate endogenous peroxidases, washed in PBS, and permeabilized with ~20 μg/ml recombinant PCR grade proteinase K (Roche) for 15 min at room temperature. The tissues were washed twice with PBS and incubated in TUNEL reaction mixture for 1 h at 37°C in a humidified chamber. Tissues were washed in PBS and labeling was detected using the Converter-POD (30 min) and DAB (5–10 min) solutions. Tissue sections were counterstained with diluted Gill #3 hematoxylin as described above.

Microarray analysis

Microarray slides containing quadruplicate spots of 521 cDNA fragments representing 366 regeneration-enriched newt genes were prepared at the Huntsman Cancer Institute Microarray Core Facility at the University of Utah. Newt limbs were either amputated or electroporated as described above and the tissues were collected at 1, 3, and 5 days postinjury and flash frozen in liquid nitrogen. Intact, nonelectroporated limbs served as controls. Limbs were pooled for each time point and ground to fine powder with a mortar and pestle while cooled in liquid nitrogen. The limb powder was transferred to Trizol (Invitrogen) and total RNA was extracted according to the manufacturer's instructions. The integrity of the total RNA was assessed by formaldehyde agarose gel electrophoresis. The RNA was amplified and purified using a RiboAmp RNA amplification procedure from Arcturus Engineering. Probes were prepared by incorporation of either Cy-3 or Cy-5 fluorescent dyes during reverse transcription of the amplified RNA templates. Hybridization was performed at 42°C for 24 h in a solution containing 50% formamide, 5× SSC, 5× Denhardt's, 0.1% SDS, and labeled probe/Cot-1 DNA (final concentration, 0.13 mg/ml) using lifter coverslips. Following hybridization, the slides were washed as follows in a series of solutions with increasing stringency: (1) 1× SSC, 0.2% SDS for 5 min at 42°C; (2) 0.1× SSC, 0.2% SDS for 5 min at 52°C; (3) 0.1× SSC, 0.2% SDS for 10 min at 52°C; and (4) four 2-min room temperature washes in 0.02× SSC. The Cy-3 and Cy-5 signals were detected by scanning the slides using a GenePix 4000B Microarray Scanner (Axon Instruments) with analysis by ImaGene 5.5 (BioDiscover, Inc.). After removing intensity data from low-quality spots, the values of remaining spots for each cDNA fragment were averaged, and log (base 2) ratios were calculated between the treated and control samples. No significant spatial variation was observed on any of the microarrays. The median intensity value for each microarray was nearly identical, so no further normalization was performed. Spots that had a signal less than 20% greater than background signal were eliminated from further analysis. Only those cDNAs that produced an appropriate signal at all three time points were included in the final analyses. The data were analyzed using Spotfire DecisionSite for Functional Genomics (Spotfire, Inc.), which allows for statistical analyses and comparison of data from multiple experiments.

Real-time RT-PCR

Reverse transcription of total RNA was performed according to manufacturer's instructions using the Bio-Rad iScript cDNA synthesis Kit and a mixture of poly-dT and random primers. Specific gene primers for real-time PCR were designed using the Beacon Designer 3.01 program (Premier Biosoft International). Sequences and amplification conditions are shown in Table 1. Real-time PCR was performed on an ABI Prism 7700 Sequence Detection System using the iTaq SYBR Green Supermix with ROX (Bio-Rad) for detection of amplified DNA. Data were analyzed using the standard curve method (Applied Biosystems, Inc.) and normalized to the control gene *histone acetyltransferase 1*. *Histone acetyltransferase 1* was selected from a group of 10 genes that had exhibited the least variation between time points based on microarray and/or northern blot analyses. Normalized values were then converted to relative values by using the intact nonelectroporated newt limb controls as the calibrator.

RNA in situ hybridization

RNA in situ hybridization was performed as previously described using antisense and sense digoxigenin-labeled riboprobes for *nCol*, *MMP3/10a*, *MMP3/10b*, and *MMP9* (Vinarsky et al., 2005).

Results

Electric fields induce dedifferentiation in intact newt limbs and tails

When newt forelimbs were subjected to five 100 ms pulses of 50 V (electric field strength = applied voltage/distance between electrodes in cm = 50V/0.3 cm = 167 V/cm), internal limb tissues

Table 1
Sequences of primers used for real-time RT-PCR

Gene	5′-Primer sequence	3′-Primer sequence
Histone acetyltransferase 1	CGTGGAGGCTGATGATATTG	GCTCGCTGACTCAATGAAC
Inositol 1,3,4,5,6-pentakisphosphate 2-kinase	ATGATGCTGGTTCAGTAGACTATG	AATCTTGCTGTCACGCTTATATTG
Profilin 2	CCGTTGGCAGGACACTCAC	GGTGGTTGGCAGTTCATTAGC
105d	TGTTCCTAGTATATTAGAGTCTG	CTGAAGAAGGCAACTAAGG
113c	GTGAGAAGGAAGTAGGATTGG	AAGATGACAGTGGTGAGAAAG
117g	TGTGTGAAGGAGGTCCTGATC	CAAACACAAGAGAGTCACAAAGTC
125c	CACAAATACGGAGAGCCCTTC	TCCCACCCTAATAATTCCCAGATC
Activating transcription factor 4	AAGTGTGAGAGTGAGGAAGAG	GTTGGGAAGGTGTATGGTTTG
Galectin 9	TCGCCGTCTGAGAACATTGC	GCGTTTACTTTATGGAGCGGAATC
Elafin-like 1	CGTTAGAGGGGTAATTCGTAAGG	ATGGATTTGTTACTTGCTATTGGG
151b	TGGTGACGCAGGAGATTATG	TGGAGTGGGAACAGTATATCG
157b	GCGGCAGACAGTAGAACTTAGC	CAGCAGGTGTAGAATCCCTCAAG
Ribosomal protein L27	GCGGCCATCGAGCTAGAC	AATCTTCTTCTTGCCCATCGTG
169e	AACTACTCACCAAGCCTCAG	ACCATGCGATCCGTTACC
Ribophorin II	CTTCTGCTTGCGGCTGTTAG	GGTCCTCAATCTCTTCCACAATG
Ras-related protein Rab 11A	AGACGACGAGTATGATTACC	CCAACAGCACCACGATAG
174a	GATGCTGACGTGACCACTGG	CCTCTGGTCTACAGGACTATTACG
193c	GCTAAAATGCCACACACAATACAG	TCGACTAAAAGCAGAAGTAGACAG
Novel 4-Apple domain gene	GCGGAATGCTGCCAGATTTAC	TGGGTCAACTGTGGACAAACG
223d	GGAGAAACCGCCACTGTGAAAG	CTTCCATCCATTCAGCCATCCATC
Variable lymphocyte receptor A	GCTTGTCATGCACTGTGGGTTC	AGAATTGGGGCGGCGAGAAG
Fc fragment of IgG binding protein	GGATGACTCTGTGGTGGTAG	GAATTGCATGTTGTTAGGTCTTG
DEAD box polypeptide 1	GGGCAACCAGAGGAGTAAATAAAG	ATCCAGATAGCATCCGACAGTG
FLN29-like gene	AACCTCCAGTATTGCTTCC	GAGTCTCTGTTGCCTGTG
MMP3/10a	CAACACACTGGAAATGATG	TCAAATGGGTAGAAGTCAC

PCR cycling conditions: initial denaturation at 95°C for 3 min; 45 cycles at 95°C for 20 s, 57°C for 20 s, and 72°C for 30 s; dissociation cycle at 95°C for 15 s, 60°C for 15 s, and 95°C for 15 s.

began to dedifferentiate in a manner resembling the dedifferentiation that occurs following limb amputation (Fig. 2). Starting at about 5 days postelectropulse, cells within the muscle tissue, periosteum, and dermal layer of the skin began to reenter the cell cycle, whereas myofibers appeared to cleave to form either smaller myofibers or mononucleated cells (Figs. 2C, E, G, I). The timing and sequence of these cellular events closely follows those events that occur during the dedifferentiation phase of limb regeneration (Figs. 2B, D, F, H). This suggests that the application of an electric field to the newt forelimb induced a dedifferentiation response in the intact limb that was histologically indistinguishable from amputation-induced dedifferentiation. The dedifferentiation response continued through at least day 14 (Figs. 2B–G), and by day 21 the myofibers were beginning to reform in the electropulsed limbs. There was still evidence of DNA synthesis in many internal cells, especially in the periosteal cells that lined the bone and in cells residing between the myofibers (Fig. 2I).

To determine whether the application of electric fields could induce a dedifferentiation response in other regeneration-competent appendages, we performed similar experiments on the newt hindlimb and tail. At day 14 postinjury, both the amputated and electrically stimulated hindlimbs and tails contained internal cells that had reentered the cell cycle as evidenced by BrdU labeling (Fig. 3). In each case, the dedifferentiation responses following amputation and electropulsing were histologically indistinguishable, suggesting that the electrically induced dedifferentiation response is universal in the regeneration-competent appendages of the newt.

Another hallmark of dedifferentiation is that markers of differentiation are down-regulated during the process (Kintner and Brockes, 1984; McGann et al., 2001; Odelberg et al., 2000), whereas blastemal markers are up-regulated (Kintner and Brockes, 1984; Onda et al., 1991). We used the myogenic differentiation marker 12/101 (Griffin et al., 1987; Kintner and Brockes, 1984) to determine whether the application of an electric field reduced the expression of this protein in newt forelimbs. Fig. 4 compares the reduction of 12/101 in amputated newt forelimbs (Fig. 4B) to the reduction observed following the application of electrical pulses (Figs. 4C–E). By day 7 postelectropulsing, there is a marked reduction in 12/101 antigen and this reduction is even more noticeable at days 10

Fig. 2. Cell cycle reentry and general histolysis in newt forelimbs following application of an electric field. Newts were injected intraperitoneally with BrdU approximately 12 h before collecting the limbs for examination. (A) An intact nonelectroporated newt limb control. Note that DNA synthesis (represented by brown nuclei that have incorporated BrdU) only occurred in the epidermal cells. (B, D, F, and H) Newt limbs were amputated and allowed to regenerate for the specified time period. Note that general histolysis of the tissues and cell cycle reentry began on day 5 postamputation and increased through regeneration days 14 to 21. (C, E, G, and I) Electric fields were applied to intact newt limbs as described in the text and limbs were examined at the specified time periods. Note that general histolysis and cell cycle reentry began on day 5 and increased through days 7 to 14. By day 21, myofibers were beginning to form again, whereas cells residing between the myofibers as well as periosteal cells continue to synthesize DNA. Arrows show examples of nuclei that were actively synthesizing DNA (B, C, I). b, bone; p, periosteal cells; m, muscle; d, dermis; e, epidermis. The scale bar in panel I is for all panels.

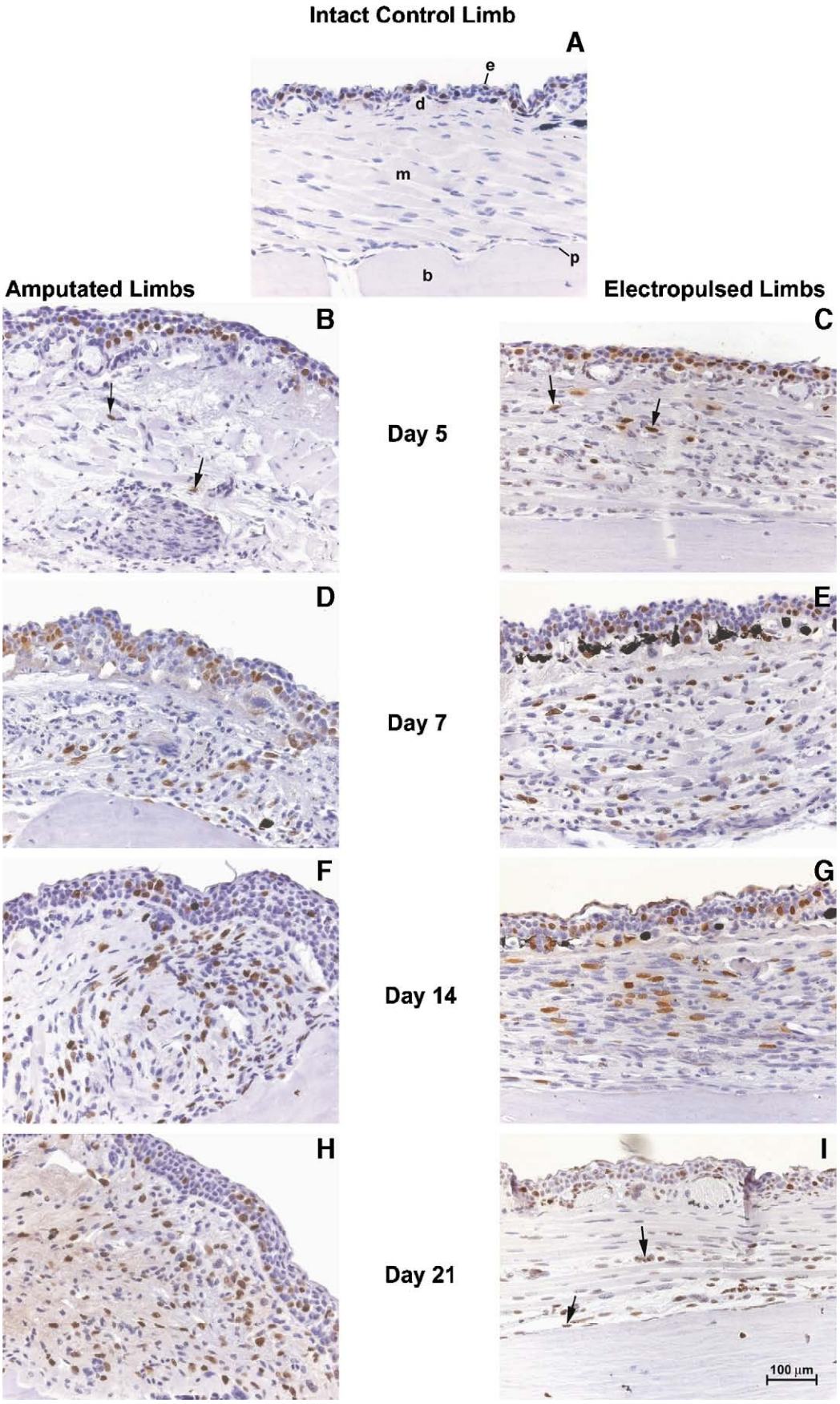
Intact Control Limb
A
e
d
m
p
b
Amputated Limbs
Electropulsed Limbs
B
C
Day 5
D
E
Day 7
F
G
Day 14
H
I
Day 21
100 µm

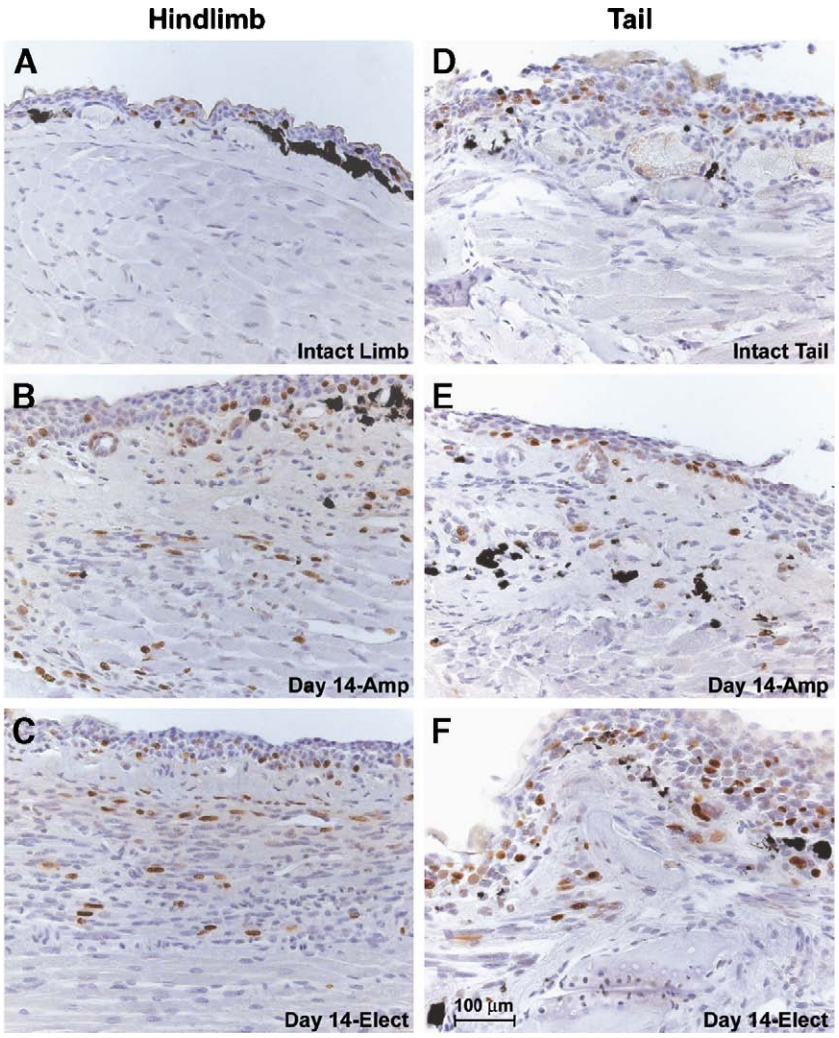

Fig. 3. Application of an electric field induces cell cycle reentry and general histolysis in newt hindlimbs and tails. (A and D) Intact, nonelectroporated hindlimb or tail control, respectively. (B and E) Hindlimb and tail, respectively, 14 days postamputation. (C and F) Hindlimb or tail, respectively, 14 days following application of an electric field. Note that cell cycle reentry and histolysis of internal appendage cells occurred following either amputation or application of an electric field. The scale bar in panel F is for all panels.

and 14. By day 21, the 12/101 marker is starting to return as the myofibers are beginning to reform (Fig. 4F), a result that is consistent with the BrdU/histolysis studies shown in Fig. 2. In contrast, the blastemal marker MT1, which is an epitope on the extracellular matrix protein tenascin (Onda et al., 1990, 1991), is up-regulated in the internal tissues within 10 days of limb amputation or electropulsing and remains up-regulated through at least day 14 (Figs. 4G–I). These results are consistent with the BrdU incorporation studies in demonstrating that the application of electric fields to newt appendages induces a dedifferentiation response.

A time course experiment using hematoxylin and eosin-stained tissue sections (Fig. 5) also demonstrated that histolysis reached a peak at 7–14 days after the application of an electric field. Breakdown of the muscle tissue is quite evident by day 7 and the number of nuclei have dramatically increased by day 14. Dermal tissues are also affected during the period of histolysis and appear to exhibit both a decrease in the number skin glands and a disorganization of the remaining glands (Figs. 5A and B). By day 21, the myofibers are starting to reform and by day 35, the electrically pulsed limbs are often indistinguishable from intact control limbs (Figs. 5E and F).

We performed TUNEL assays and searched for signs of necrotic myofibers to determine whether the apparent dedifferentiation events following the application of an electric field were associated with increases in cell death due to apoptosis or necrosis (Fig. 6). The TUNEL assays revealed the presence of only a few apoptotic cells following either amputation or application of an electric field (Figs. 6A–D) and histological examination showed no evidence of necrosis, such as weak cytoplasmic staining with eosin or the infiltration of macrophages or other leukocytes (Fig. 6E). During the breakdown of the myofibers, many of the resulting cells contained a single nucleus surrounded by cytoplasm that stained brightly with eosin. Mitotic figures were also observed during myofiber breakdown. As shown above, myofiber nuclei reentered the cell cycle (Figs. 2 and 3) and some myofibers continued to express the 12/101 marker during the early stages

of cleavage (Figs. 4C and D). In addition, the blastemal marker MT1 was up-regulated during the dedifferentiation process (Figs. 4G–I). These indicators of cell survival and growth during the early stages of electrically induced histolysis are inconsistent with marked cell necrosis. Instead, our results strongly suggest that electrical pulses delivered to intact newt limbs initiate a dedifferentiation response that is histologically and cellularly indistinguishable from the response elicited by limb amputation.

Correlation between electroporation and dedifferentiation

If the strength of an electric field reaches a certain threshold, it can produce the formation of transient pores in the cell

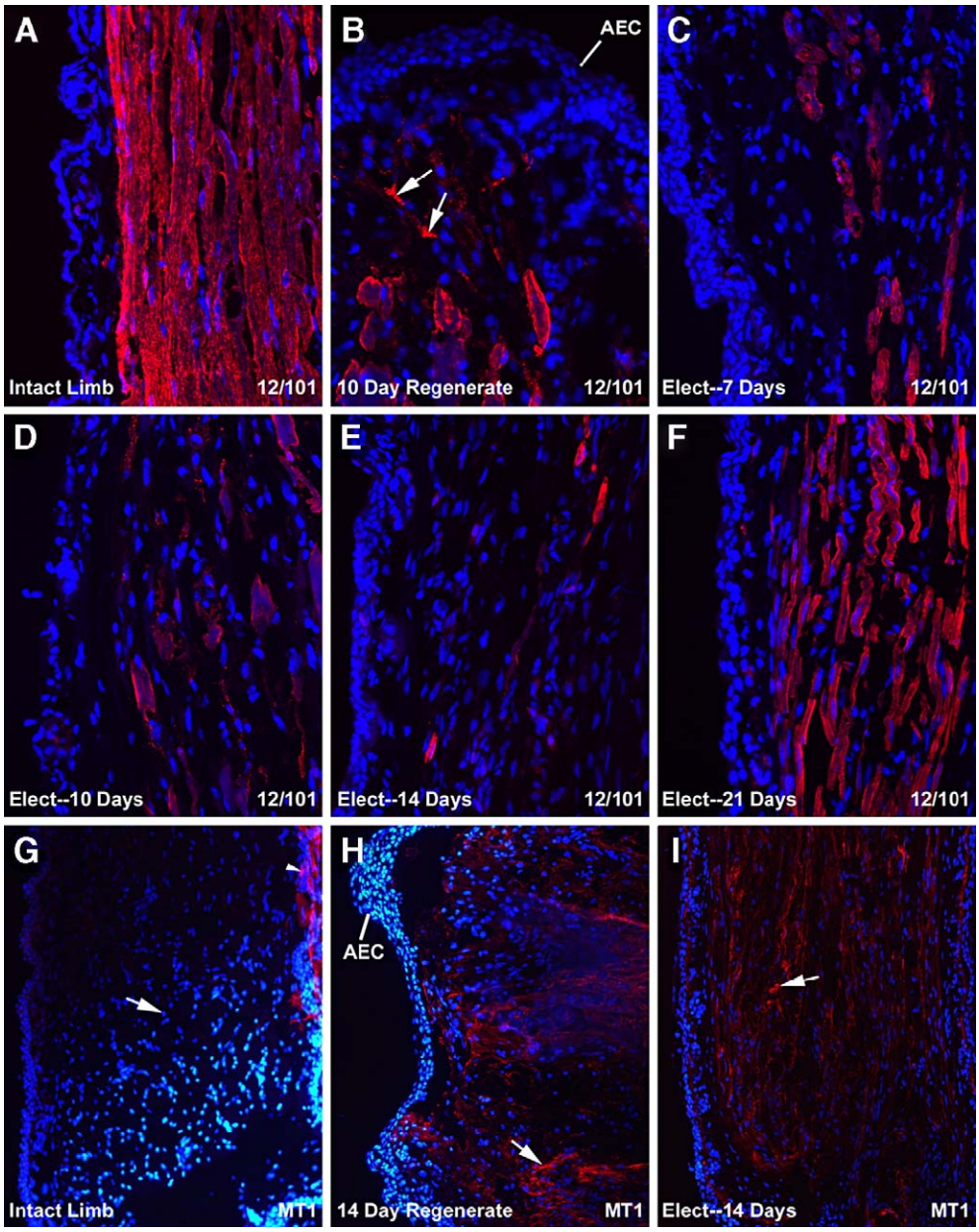

Fig. 4. Regulation of muscle differentiation and blastemal markers following the application of an electric field to newt forelimbs. (A) Immunofluorescence assay on intact nonelectroporated control limbs demonstrated high expression of 12/101 in myofibers (red fluorescence). Tissue counterstained with DAPI to show nuclei (blue fluorescence). (B) Limb regenerate 10 days postamputation. Note the reduction in 12/101 fluorescence in cells proximal to the apical epithelial cap (AEC). The fluorescing cells also appear to be fragmenting to form smaller cells (arrows). (C–F) Intact electroporated limbs at 7, 10, 14, and 21 days following the application of an electric field. Note the marked reduction of 12/101 expression and that some cells continue to express the 12/101 antigen during myofiber cleavage and histolysis (C–E). By day 21, myofibers were starting to reform and there was a concomitant increase in 12/101 expression (F). (G) Immunofluorescence assay of an intact nonelectroporated control limb demonstrated no expression of tenascin (MT1 epitope, red fluorescence) in the muscle tissues (arrow), a result consistent with previous studies (Onda et al., 1990, 1991). However, other tissues, such as the epidermis, tendons, and periosteum express tenascin in intact limbs and presumably the positive signal in the upper right hand corner of the panel represents such tissues (arrowhead). (H) Limb regenerate 14 days postamputation. Note the increase in MT1 fluorescence in the late dedifferentiation/early blastemal tissues (arrow). (I) An intact electroporated limb 14 days following the application of an electric field. Note the increase in MT1 fluorescence in the dedifferentiating myofibers (arrow).

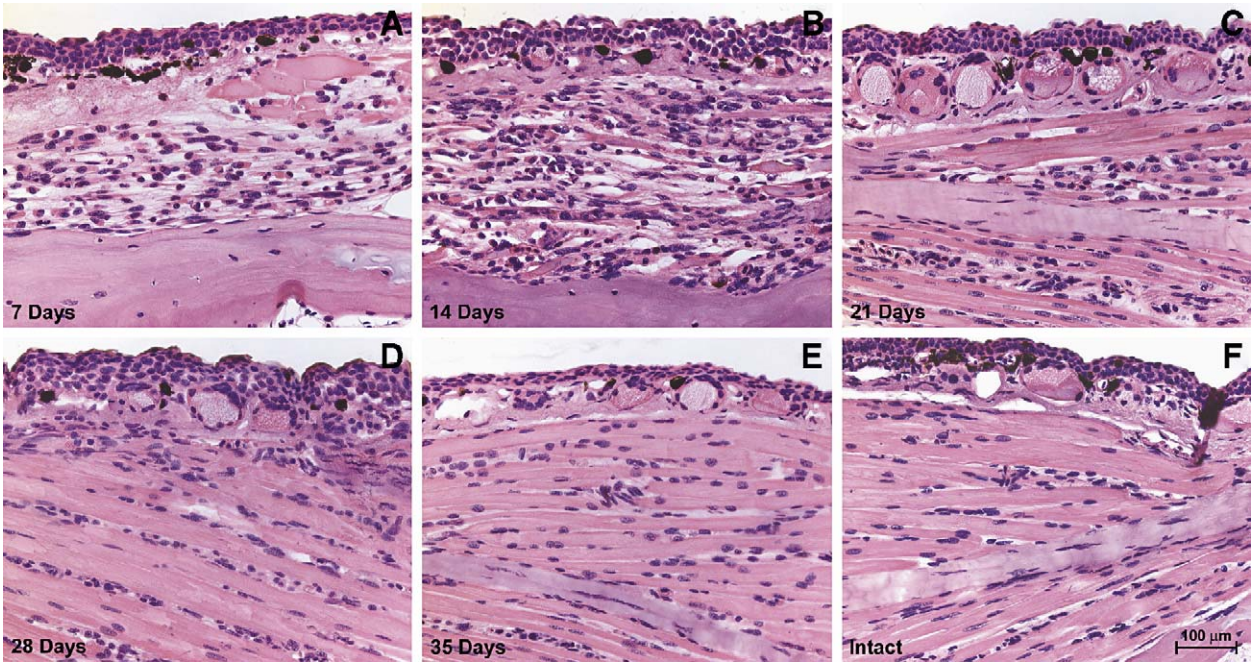

Fig. 5. A time course for complete regeneration of tissue structure following application of an electric field. Hematoxylin and eosin-stained tissue sections from newt forelimbs were taken at weekly intervals following the application of an electric field. (A and B) Note that histolysis of muscle and dermal tissues (including skin glands) was prevalent 7 and 14 days post electrical stimulation. (C and D) By days 21 and 28, myofibers and skin glands were starting to reform. (E) By day 35, the histology of the tissues was often indistinguishable from the intact, nonelectroporated control (F). Scale bar shown in panel F is for all panels.

membrane, a process known as electroporation. Electroporation is often used to deliver molecules such as DNA into cells. During the electrical pulse, the negatively charged DNA molecules will be driven towards the anode and through pores that have formed in the cell membranes. This electrophoretic effect has been shown to be essential for efficient DNA transfection, given that DNA plasmids added after the administration of the electrical pulse but before closure of the transient pores do not transfect cells (Golzio et al., 2002; Mir et al., 1999; Sukharev et al., 1992). The existence of the transient pores can be measured in minutes. For example, in mouse and rat myofibers, most of these pores have resealed in about 9 min (Bier et al., 1999; Gehl et al., 2002).

To determine whether electroporation of limb cells was required for the dedifferentiation process, we injected newt limbs with an EGFP expression construct and applied five electrical pulses at varying electrical field strengths ranging from 33 V/cm to 167 V/cm. We were able to observe very low levels of EGFP expression when electric field strengths reached 67 V/cm and the expression levels increased as the electric fields increased to 167 V/cm, indicating that electroporation of the limb cells begins at electric field strengths of about 67 V/cm and increases with the application of higher electric field strengths (Figs. 7A, C, and E). When we performed BrdU incorporation assays on either the same limbs or other limbs pulsed with equivalent voltages, we observed cell cycle reentry in the periosteal and muscle cells starting at electric fields of 67 V/cm and increasing in number as the strength of the electric fields increased to 167 V/cm (Figs. 7B, D, and F). Myofiber breakdown was apparent at the higher electric field strengths, but not at 67 V/cm. The correlation between electric field strengths required to produce electroporation as measured by transgene expression and those required to induce a dedifferentiation response suggests that the minor and transient injury that occurs in cells following application of a series of electrical pulses is sufficient to induce the genetic programs that regulate dedifferentiation in the newt.

Analysis of temporal gene expression during amputation- and electroporation-induced dedifferentiation

Given that the dedifferentiation responses following amputation and electroporation were indistinguishable at the histological and cellular levels, we next examined whether the two processes were defined by similar gene expression profiles. Similar profiles would strongly suggest that both types of dedifferentiation are controlled by the same molecular signals and pathways. For these studies, we examined gene expression at three different time points following newt forelimb amputation or electroporation. The time points chosen were 1, 3, and 5 days post-injury. By performing microarray analyses on amputated and electroporated newt forelimbs using an in-house regeneration-enriched cDNA chip, we found that 153 of 203 genes (75.4%) exhibited similar expression patterns (less than 2-fold difference) at all three time points following either amputation or electroporation, whereas only 7 genes (3.4%) exhibited greater than 2-fold difference in expression at all three time points. Of these 153 genes, 35 (22.9%) were up- or down-regulated at least a 2-fold when compared to intact limbs (Table 2). Using the less stringent criterion where expression data between the two types of injury models only had to match (less than 2-fold difference) at two of three time points, 175 of

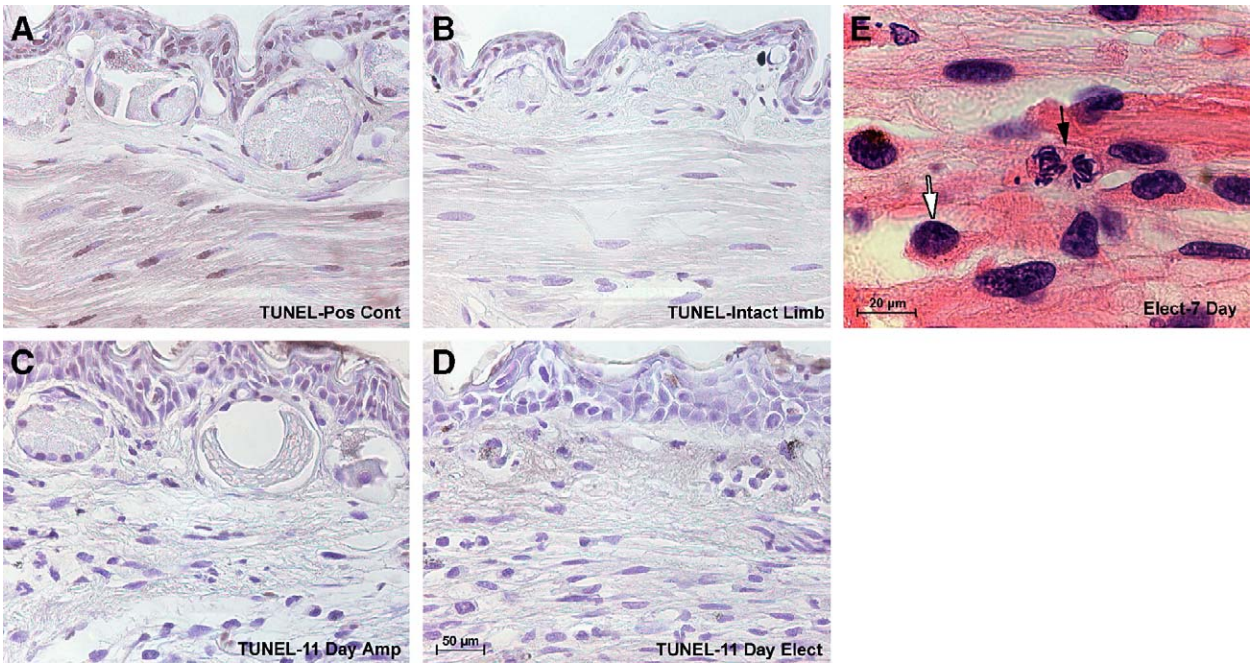

Fig. 6. Application of low level electric fields causes little cell death in newt forelimbs. TUNEL assays were performed to assess level of apoptosis following application of an electric field. Brown nuclei represent cells positive for the TUNEL assay, whereas nonapoptotic nuclei are blue. (A) Positive control for apoptosis. Tissue section was treated with DNase I to create strand breaks before performing the TUNEL assay. (B) Intact, nonelectroporated control newt limb. Very few, if any, cells were TUNEL positive. (C) Limb regenerate 11 days postamputation. Only a few cells were TUNEL positive. (D) Intact newt limb 11 days following application of an electric field. Very few, if any, cells were TUNEL positive. (E) High-powered examination of hematoxylin and eosin-stained tissue sections of newt limbs 7 days following the application of an electric field revealed no evidence of necrosis. However, evidence for cell survival and growth were present in the tissues undergoing histolysis. Black arrow denotes a mitotic cell in late anaphase or early telophase. White arrow points to a healthy mononucleated cell with bright-staining cytoplasm. Scale bar in panel D is for panels A–D.

203 (86.2%) genes were deemed to have similar expression patterns.

In some cases, genes that were highly up-regulated following both amputation and electroporation did not meet our stringent criteria for inclusion because either electroporation or amputation induced a greater than 2-fold difference in the level of expression between the two types of injuries. For example, *MMP9*, which was highly up-regulated following both types of injuries, exhibited a much higher level of expression following electroporation than amputation at two of the three time points, whereas *MMP3/10a* exhibited higher expression at one of the three time points. Therefore, these genes were not included in Table 2, although their expression patterns suggest that they play important roles in the response to both types of injuries. All 7 genes that showed markedly different expression patterns were expressed at much higher levels following limb amputation than following electroporation, suggesting that they either might be involved in wound closure or be regulated by physiological conditions that normally follow amputation, such as hypoxia.

Of the 35 genes that exhibited similar expression patterns between the two types of injuries, 19 of them could be placed into known gene or EST families based on sequence analysis. The remaining 16 genes fell into one of three categories: (1) genes that were novel; (2) genes of unknown function; or (3) cDNAs that were too short to make any assignments. Of the 19 known genes, 3 encoded proteases with 2 of these, *nCol* (AY857753) and *MMP3/10b* (AY857754), belonging to the matrix metalloproteinase (MMP) family and the remaining gene being the cysteine protease cathepsin L. As noted above, two additional MMP genes, *MMP3/10a* (AY857751) and *MMP9* (AY857752), were also highly up-regulated following both amputation and electroporation but did not meet our criteria for inclusion. Some of the other known genes encode protease inhibitors, receptors, antimicrobial proteins, and putative anti-inflammatory agents.

The seven genes exhibiting markedly different expression patterns between the two injury models make up a mixed group encoding the muscle proteins parvalbumin, cardiac α-actin, troponin C, and genes that can be up-regulated by hypoxia, including those encoding the glycolytic enzymes enolase 3 or 1 and fructose-bisphosphate aldolase I (Discher et al., 1998; Ferry et al., 1983; Kouno et al., 2000; Semenza et al., 1996). The up-regulation of hypoxia-induced genes following amputation is consistent with previous studies that have shown a decrease in the number of blood vessels just proximal to the amputation plane during the first week following limb amputation (Peadon and Singer, 1966; Rageh et al., 2002; Smith and Wolpert, 1975). We have observed no such decrease in the number of blood vessels following electroporation and therefore would not expect to observe hypoxia-induced gene up-regulation in electroporated limbs.

Real-time RT-PCR on a selected group of 24 genes (*histone acetyltransferase 1* was used as the control gene—see Materials and methods) confirmed the results of the microarray analyses

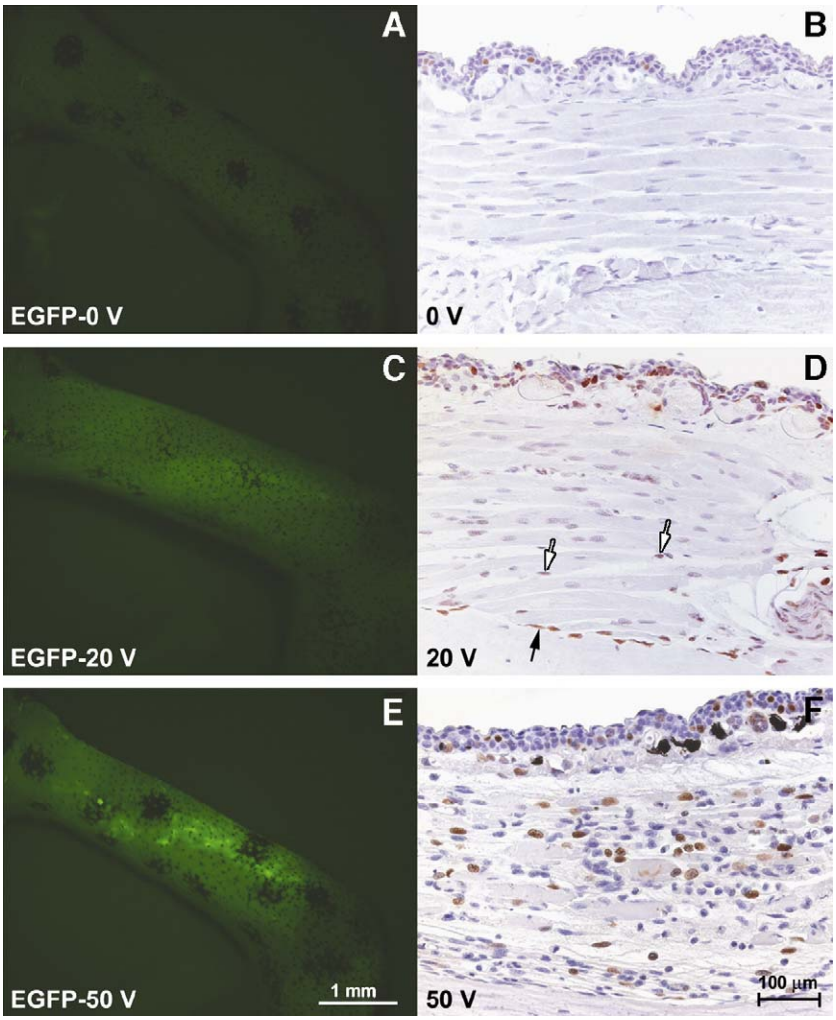

Fig. 7. Dedifferentiation correlates with electric field strengths sufficient to cause electroporation of cell membranes. Newt limbs were injected with an EGFP expression construct followed by the application of electrical pulses at varying electric field strengths. EGFP expression was monitored 7 days following application of the electric field and cell cycle reentry and histolysis were examined. (A and B) No electrical pulses were given following injection. No EGFP expression or cell cycle reentry was observed. (C and D) Five 20 V (Electric field strength = 67 V/cm), 100 ms pulses were delivered to the newt forelimb. Low levels of EGFP expression were observed and a few internal cells, mostly periosteal cells (black arrow) but also some muscle cells (white arrows) have reentered the cell cycle. Very little histolysis was observed. (E and F) Five 50 V (Electric field strength = 167 V/cm), 100 ms pulses were delivered to the newt forelimb. Expression of EGFP was abundant and both cell cycle reentry and histolysis of the tissues were observed. Scale bar in panel E is for panels A, C, and E. Scale bar in panel F is for panels B, D, and F.

while giving us a more dynamic assessment of the degree of differential expression for these selected genes (Yuen et al., 2002). For this analysis, we chose both genes that exhibited marked up-regulation following injury as well as genes that showed very little variation in expression levels. The 11 genes that exhibited at least a 2-fold up-regulation following both electroporation and amputation when analyzed by microarray analysis were also shown to be up-regulated more than 2-fold by real-time RT-PCR (first 11 genes in Table 3), whereas the 10 genes that exhibited little change in expression by microarray analysis also showed little variability when analyzed by real-time RT-PCR (last 10 genes in Table 3). There were small discrepancies between the microarray and real-time RT-PCR results for 3 of the 24 genes. For *174a*, microarray analysis detected a small increase (<2-fold) in mRNA levels following amputation and a >2-fold increase following electroporation. Real-time RT-PCR, however, showed that *174a* is up-regulated >2-fold following both types of injuries, a result that is consistent with northern blot analysis (data not shown). Microarray analysis indicated that *193c* and *profilin 2* were up-regulated >2-fold following amputation but did not reach this threshold following electroporation. However, real-time RT-PCR demonstrated that both of these genes were up-regulated >2-fold following both types of injuries. These results suggest our microarray data provide conservative estimates for the degree of differential expression following limb injury. Therefore, any gene we identify as being up- or down-regulated by at least 2-fold by microarray analysis is likely to be differentially expressed.

Real-time RT-PCR also revealed underlying differences in the differential expression levels of some genes following amputation or electroporation. However, when these differences occurred, they were often due to a slight shift in the timing of gene expression. For example, *MMP3/10a* exhibited

Table 2
Differentially expressed genes that exhibited similar or markedly different differential expression patterns following amputation and electroporation as determined by microarray analysis

Similar expression patterns	Markedly different expression patterns
Genes placed in known families	
nCol	Enolase 3 or 1
MMP3/10b	Cardiac α-actin
TIMP1	Parvalbumin
Cathepsin L	Fructose-bisphosphate aldolase I
Galectin 9	Troponin C, fast skeletal
Complement component C1qα	
Ferritin, heavy polypeptide 1	
Immune responsive protein 1	
Variable lymphocyte receptor A	
Neutrophilic granule protein-like gene	
Interferon regulatory factor I	
Peptidoglycan recognition protein	
Fc fragment of IgG binding protein	
Ribosomal protein S3	
Urokinase-type plasminogen activator receptor	
Elafin-like 1	
Profilin 2	
Novel 4 apple domain gene	
ATP synthase, F0, subunit f iso 2	

Genes that cannot be placed in known families		
12b	97c4	224c
196d	109c3	177c
264e	151b	
223d	178d13	
185at11	101b	
174a	125c	
161d	157b	
56c	117g	

very high levels of gene expression within 1 day of limb amputation or electroporation. By day 3, the levels had dropped considerably in the amputated limbs but remained very high following electroporation. By day 5, however, expression levels were greatly reduced in both injury types. Whether these differences in temporal expression have biological significance has yet to be determined.

Analysis of spatial gene expression during amputation- and electroporation-induced dedifferentiation

To further compare the dedifferentiation responses between amputated and electroporated limbs, we examined spatial expression patterns of selected genes in the two injury model systems. We have previously demonstrated that matrix metalloproteinases (MMPs) are required for normal newt limb regeneration and that at least three different MMPs, *nCol*, *MMP3/10b*, and *MMP9* are up-regulated in the internal limb tissues that undergo dedifferentiation during the early stages of limb regeneration (Vinarsky et al., 2005). To determine whether these genes are up-regulated in the same tissues following electroporation, we performed RNA in situ hybridization on limb tissue sections at days 1, 3, and 5 postelectroporation and compared the spatial expression patterns to those observed in amputated limbs (Fig. 8). *nCol* and *MMP9* were expressed in the periosteum and epithelia (skin and/or apical epithelial cap) following both types of injuries, whereas *MMP3/10b* was expressed in the epithelium and in the muscle tissues that will be undergoing dedifferentiation. *MMP9* was also expressed in the endosteal cells following either amputation or electroporation. The common spatial expression patterns of these important regeneration genes further strengthens the argument that amputation- and electroporation-induced dedifferentiation are nearly identical processes controlled by the same genetic program.

Discussion

We present evidence demonstrating that electric fields sufficient to cause electroporation of newt limb cells can induce a dedifferentiation response in limbs and tails that is virtually indistinguishable at the histological and molecular levels from the dedifferentiation response following appendage amputation. The data suggest that dedifferentiation is most likely a result of the widespread, but transient opening of pores in the cell membrane following the application of the electric field. This minor, transient injury is apparently sufficient to initiate the genetic program that leads to the dedifferentiation of cells in the injured appendage. We reach this conclusion based on the correlation between the electric field strength required to induce both dedifferentiation and electroporation. An alternative explanation would be that the electric fields themselves might induce this response either by activating ion channels directly or by releasing growth factors and cytokines from the extracellular matrix (ECM). These signals could then lead to the activation or repression of downstream genes that regulate the dedifferentiation response. The ion channel hypothesis would be consistent with previous work demonstrating the importance of electrical current and sodium ion channels during the initial stages of limb regeneration (Borgens et al., 1979; Jenkins et al., 1996), whereas the release of cytokines from the ECM following electrical stimulation has been demonstrated for other systems (Braunhut et al., 2004; Zhou et al., 1998). These latter explanations would be satisfying because they could help bridge the gap between two historically different ways of viewing the initiation of salamander limb regeneration, i.e., through the regulation of genes or through currents controlled by ion channels.

Although the dedifferentiation processes following amputation and electroporation are nearly indistinguishable, only amputation leads to the regrowth of a new appendage. This suggests that the signals required for appendage outgrowth and/or patterning of a new limb are not present following electroporation. Instead, the minor and transient injury caused by the electrical pulses induce a robust dedifferentiation response that the newt efficiently resolves by regenerating the normal internal tissues of the original appendage. This regenerative process is similar to the response that is observed following a mild crush injury in larval axolotls (Mescher, 1982) and appears to be an efficient method for regenerating tissues following an injury that does not involve the complete loss of an

Table 3
Relative differential expression of selected genes following amputation and electroporation as determined by real-time RT-PCR

Gene	Day 1		Day 3		Day 5	
	Amp	Elect	Amp	Elect	Amp	Elect
MMP3/10a	42.3±13.0	117.5±9.1	4.0±1.8	46.3±20.7	4.7±1.2	1.9±0.3
169e	40.7±8.6	30.1±5.4	6.9±1.4	8.6±1.2	2.5±0.5	8.3±1.0
Fc Fragment of IgG binding protein	29.2±3.8	2.8±0.8	34.1±5.2	28.7±4.9	6.3±2.3	38.1±17.3
223d	28.4±3.7	20.1±2.2	10.6±3.8	14.6±1.4	3.8±0.6	6.6±0.7
151b	8.6±1.5	17.9±2.5	6.7±1.2	8.3±1.8	7.6±1.8	4.5±0.4
Galectin 9	15.6±4.8	9.7±1.9	16.5±3.7	6.6±2.8	32.0±6.1	5.7±1.4
Elafin-like 1	12.1±1.6	8.6±1.2	13.6±0.8	17.0±1.5	1.2±0.1	7.8±0.8
157b	4.7±0.7	9.6±1.0	9.1±0.7	9.2±1.0	3.1±0.4	4.0±0.4
125c	5.8±1.2	10.5±1.1	9.1±1.1	7.4±0.9	5.0±0.6	3.7±0.5
4 Apple domain protein	11.4±1.6	6.2±0.7	2.2±0.1	2.1±0.3	8.7±0.9	1.0±0.1
Variable lymphocyte receptor A	1.5±0.2	3.1±0.4	8.4±0.6	5.9±0.5	2.0±0.3	4.8±0.4
174a	5.9±1.2	13.7±1.5	7.9±0.9	14.5±1.3	3.5±0.4	6.3±0.5
193c	0.3±0.0	2.4±0.3	3.4±0.6	5.4±0.5	0.6±0.1	3.9±0.3
Profilin 2	2.0±0.3	2.6±0.2	3.8±0.1	2.0±0.2	2.4±0.2	1.9±0.2
117g	0.7±0.1	2.5±0.5	0.9±0.2	0.7±0.2	0.9±0.1	0.4±0.1
FLN29-like gene	1.8±0.2	3.0±0.2	0.7±0.3	1.5±0.3	1.7±0.2	1.0±0.2
Activating transcription factor 4	2.7±0.5	2.7±0.3	1.8±0.3	1.5±0.2	2.0±0.3	1.4±0.1
Ribophorin II	2.9±0.6	2.2±0.2	1.7±1.1	1.1±0.3	2.8±0.6	1.1±0.5
DEAD box polypeptide 1	0.8±0.3	2.2±0.3	0.2±0.2	1.2±0.4	1.1±0.0	1.0±0.1
Ras-related protein Rab 11A	1.9±0.7	1.4±0.4	2.1±1.0	1.4±1.0	1.5±0.3	1.3±1.0
Inositol 1,3,4,5,6-pentakisphosphate 2-kinase	1.0±0.4	1.3±0.4	1.0±0.5	1.0±0.2	0.7±0.3	1.0±0.2
113c	1.0±0.1	1.5±0.5	1.0±0.2	1.1±0.4	0.7±0.1	1.2±0.2
105d	0.7±0.2	0.8±0.4	1.3±0.2	1.2±0.6	0.7±0.2	0.9±0.2
Ribosomal protein L27	0.3±0.0	0.7±0.1	0.7±0.1	0.7±0.1	0.3±0.0	0.6±0.1

Numbers represent *x*-fold up-regulation following amputation (Amp) or electroporation (Elect). Standard deviations for each of these values are shown. Values were normalized to the *histone acetyltransferase 1* gene.

appendage. In contrast, a different result can occur when the injury is more severe and involves the severing and deviation of the brachial nerves, removal of large patches of skin, and the destruction of muscle tissue. When such injuries are located near the shoulder, newts often respond by growing supernumerary limbs (Bodemer, 1958, 1959). Supernumerary limbs can also be produced at the site of limb wounds by combining nerve transection and deviation with the juxtaposition of two pieces of skin with opposite axial limb polarities (Endo et al., 2004; Lheureux, 1977; Maden and Mustafa, 1984; Reynolds et al., 1983). The insertion of carcinogenic microcrystals into connective tissues beneath the surface of the skin on the newt forelimb can occasionally induce supernumerary limb formation (Tsonis and Eguchi, 1981). Presumably, the induction of the new limb is a result of the injury created by the insertion of the microcrystal through the skin coupled with the extended effects of the carcinogen.

Another study has recently presented evidence suggesting that the combination of plasmid injection and application of an electric field to axolotl tail myofibers can induce dedifferentiation in 5–10% of the electroporated axolotl myofibers (Schnapp and Tanaka, 2005). In the present study, we demonstrate that the application of an electric field to newt appendages in the absence of any other injury, such as injection, can induce widespread dedifferentiation that is indistinguishable from the response observed following limb amputation. Our results also suggest that limb tissues may be more susceptible to the effects of electroporation than tail tissues (compare Figs. 2 and 3) and this difference might explain, at least in part, the low percentage of tail myofibers that dedifferentiated in the axolotl study. Other explanations might include species differences in the response to electrical stimulation and differences in methodology.

Our gene expression studies revealed several potential dedifferentiation/cellular plasticity genes, including four members of the MMP family. Two of these genes, *nCol* and *MMP3/10b*, exhibited comparable differential expression patterns between amputated and electroporated forelimbs at all time points examined, whereas the other two genes, *MMP9* and *MMP3/10a*, were highly up-regulated following both types of injuries but exhibited significantly higher expression levels at one or more time points in intact electroporated limbs. We have previously demonstrated that MMP function is required for normal newt limb regeneration and that *nCol*, *MMP3/10b*, and *MMP9* are expressed in the early stages of regeneration in tissues that will undergo dedifferentiation (Vinarsky et al., 2005). In this study, we show that following the application of an electric field these same MMP genes are also expressed in tissues that will be undergoing dedifferentiation. These results further support the hypothesis that the MMP genes are involved in the dedifferentiation process. Whether MMPs play an active role in this process by either activating signaling proteins or releasing dedifferentiation-initiating cytokines from the extracellular matrix (ECM) or whether they play a more permissive role by remodeling the ECM has not yet been determined.

Finally, this study indicates that caution must be exercised when interpreting results where electroporation has been used in

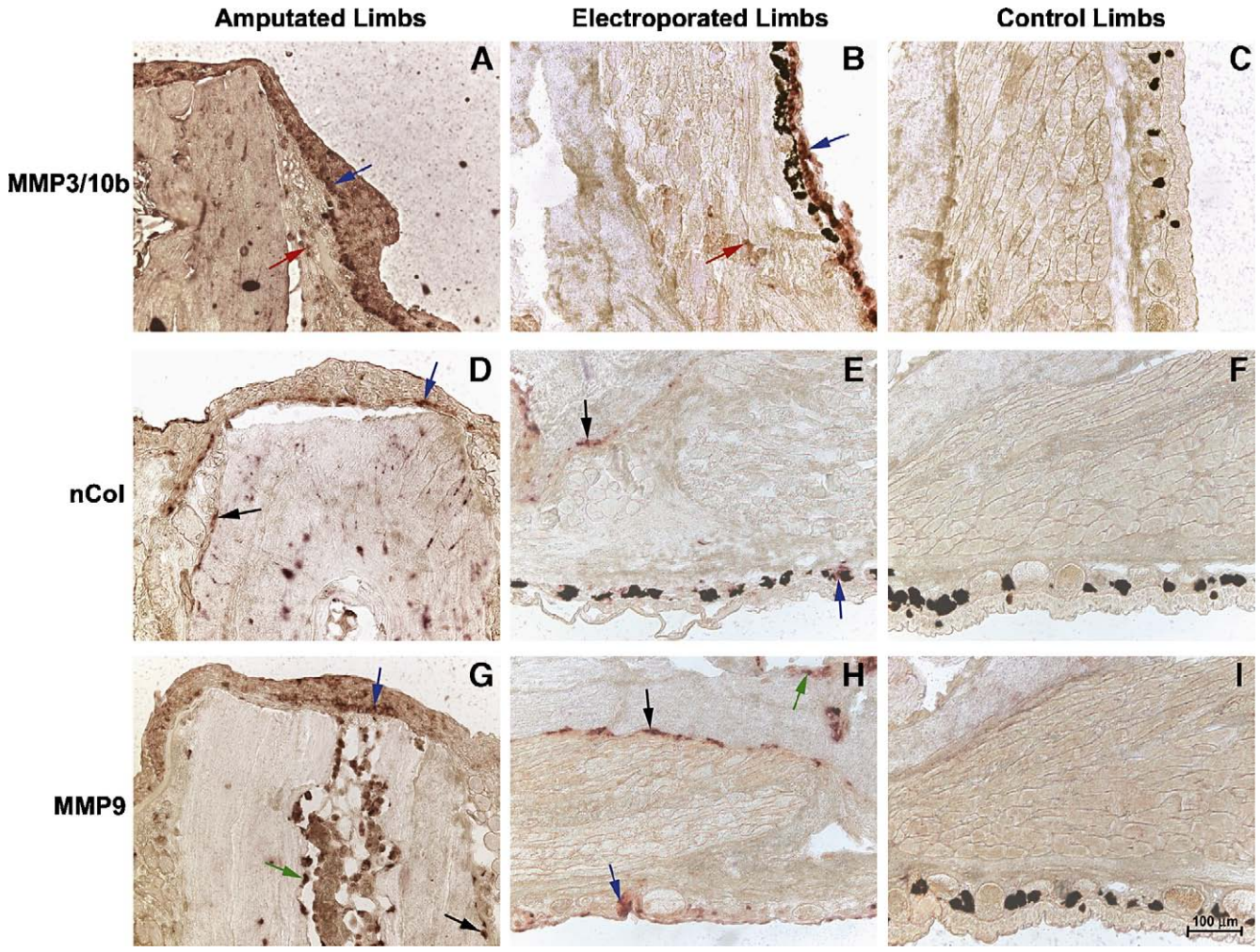

Fig. 8. Spatial expression patterns of up-regulated genes are similar following amputation or electroporation. RNA in situ hybridization of amputated and electroporated forelimb using riboprobes directed towards three MMP genes revealed that these genes were expressed in similar tissues following amputation or electroporation. Arrows point to areas of MMP expression: blue arrows, epithelium; black arrows, periosteum; red arrows, muscle; green arrows, endosteum. MMP denote MMP expression in the epidermis, black arrows point to MMP expression in the periosteum denote areas of MMP expression. (A–C) *MMP3/10b* antisense probe hybridized to a 1-day limb regenerate (A), an intact limb 1 day postelectroporation (B), and intact, nonelectroporated control limb (C). Expression was observed in the basal layer of the AEC or epidermis and in the muscle tissues of the stimulated limbs, but not the control. (D–F) *nCol* antisense probe hybridized to a 5-day limb regenerate (D), an intact limb 1 day postelectroporation (E), and intact, nonelectroporated control limb (F). Expression was observed in the basal layer of the AEC or epidermis and periosteal cells of the stimulated tissues, but not in the control. (G–I) *MMP9* antisense probe hybridized to a 1-day limb regenerate (G), an intact limb 1 day postelectroporation (H), and intact, nonelectroporated control limb (I). Expression was observed in the basal layer of the AEC or epidermis, periosteal cells, and endosteal cells but not the control. Control sense probes did not hybridize to tissue sections taken from the same limbs (data not shown). Scale bar shown in panel I is for all panels.

vivo for transfecting expression constructs. This is especially true if the experiments are designed to examine various aspects of cellular plasticity, e.g., dedifferentiation, cell cycle reentry, or multipotency. Such responses could be a consequence of gene activation by cellular electroporation, rather than the effects of transgene expression. Caution is also warranted in cases where the transgene acts only as a marker for following cell fate, given that electroporation might affect the potency of the transfected cell(s). In future in vivo studies involving electroporation, it will be important to implement controls that assess the effects of electroporation alone.

In conclusion, our data demonstrate that application of an electric field sufficient to induce transient electroporation of cell membranes induces a dedifferentiation response that is virtually indistinguishable from the response that occurs following amputation of newt appendages. This discovery allows us to predict whether a gene that is differentially expressed following amputation will likely function in the dedifferentiation process. It also provides a possible method for determining whether a gene is required for dedifferentiation by knocking down its function in intact newt appendages using electroporation-delivered morpholinos or RNA interference.

Acknowledgments

We would like to thank George Eisenhoffer, Alejandro Sanchez Alvarado, Nestor Oviedo, and Kevin Flanigan for helpful suggestions and Brian Dalley and the Huntsman Microarray Core Facility for their technical assistance with the

microarray analyses. We also thank David Kent and Katherine Zukor for technical assistance. This work was funded by grants from the National Institute of Neurological Disorders and Stroke (Grant Numbers R01 NS043878 and R01 NS043878S) (SJO).

References

Bier, M., Hammer, S.M., Canaday, D.J., Lee, R.C., 1999. Kinetics of sealing for transient electropores in isolated mammalian skeletal muscle cells. Bioelectromagnetics 20, 194–201.

Bodemer, C.W., 1958. The development of nerve-induced supernumerary limbs in the adult newt, *Triturus viridescens*. J. Morphol. 102, 555–582.

Bodemer, C.W., 1959. Observations on the mechanism of induction of supernumerary limbs in adult *Triturus viridescens*. J. Exp. Zool. 140, 79–99.

Bodemer, C.W., Everett, N.B., 1959. Localization of newly synthesized proteins in regenerating newt limbs as determined by radioautographic localization of injected methionine-S^{35}. Dev. Biol. 1, 327–342.

Borgens, R.B., Vanable Jr., J.W., Jaffe, L.F., 1979. Reduction of sodium dependent stump currents disturbs urodele limb regeneration. J. Exp. Zool. 209, 377–386.

Braunhut, S.J., McIntosh, D., Vorotnikova, E., Zhou, T., Marx, K.A., 2004. Development of a smart bandage: applying electrical potential to selectively release wound healing growth factors from cell free extracellular matrices. Material Research Society Journal 711, 1–3.

Breedis, C., 1952. Induction of accessory limbs and of sarcoma in the Newt (*Triturus viridescens*) with carcinogenic substances. Cancer Res. 12, 861–866.

Brockes, J.P., Kumar, A., 2002. Plasticity and reprogramming of differentiated cells in amphibian regeneration. Nat. Rev., Mol. Cell Biol. 3, 566–574.

Butler, E.G., Ward, M.B., 1967. Reconstitution of the spinal cord after ablation in adult Triturus. Dev. Biol. 15, 464–486.

Chalkley, D.T., 1954. A quantitative histological analysis of forelimb regeneration in *Triturus viridescens*. J. Morphol. 94, 21–70.

Della Valle, P., 1913. La doppia rigenerazione inversa nella fratture della zampe di Triton. Boll. Soc. Nat. Napoli 25, 95–160.

Discher, D.J., Bishopric, N.H., Wu, X., Peterson, C.A., Webster, K.A., 1998. Hypoxia regulates beta-enolase and pyruvate kinase-M promoters by modulating Sp1/Sp3 binding to a conserved GC element. J. Biol. Chem. 273, 26087–26093.

Endo, T., Bryant, S.V., Gardiner, D.M., 2004. A stepwise model system for limb regeneration. Dev. Biol. 270, 135–145.

Ferry, J.A., Nichols, R.C., Condon, S.J., Stubbs, J.D., Bowen, S.T., 1983. Artemia hemoglobins. Increase in net synthesis of the beta-polypeptide (relative to the alpha-polypeptide) in hypoxia. Biochim. Biophys. Acta 739, 249–257.

Gehl, J., Skovsgaard, T., Mir, L.M., 2002. Vascular reactions to in vivo electroporation: characterization and consequences for drug and gene delivery. Biochim. Biophys. Acta 1569, 51–58.

Golzio, M., Teissie, J., Rols, M.P., 2002. Direct visualization at the single-cell level of electrically mediated gene delivery. Proc. Natl. Acad. Sci. U. S. A. 99, 1292–1297.

Griffin, K.J., Fekete, D.M., Carlson, B.M., 1987. A monoclonal antibody stains myogenic cells in regenerating newt muscle. Development 101, 267–277.

Hay, E.D., Fischman, D.A., 1961. Origin of the blastema in regenerating limbs of the newt *Triturus viridescens*. An autoradiographic study using tritiated thymidine to follow cell proliferation and migration. Dev. Biol. 3, 26–59.

Jenkins, L.S., Duerstock, B.S., Borgens, R.B., 1996. Reduction of the current of injury leaving the amputation inhibits limb regeneration in the red spotted newt. Dev. Biol. 178, 251–262.

Kintner, C.R., Brockes, J.P., 1984. Monoclonal antibodies identify blastemal cells derived from dedifferentiating limb regeneration. Nature 308, 67–69.

Kouno, A., Inoue, H., Bajanowski, T., Maeno, Y., Iwasa, M., Nakayama, M., Nishi, K., Brinkmann, B., Matoba, R., 2000. Development of haemoglobin subtypes and extramedullary haematopoiesis in young rats. Effects of hypercapnic and hypoxic environment. Int. J. Legal Med. 114, 66–70.

Lheureux, E., 1977. Importance of limb tissue associations in the development of nerve-induced supernumerary limbs in the newt *Pleurodeles waltlii* Michah (author's transl). J. Embryol. Exp. Morphol. 38, 151–173.

Maden, M., Mustafa, K., 1984. The cellular contributions of blastema and stump to 180 degrees supernumerary limbs in the axolotl. J. Embryol. Exp. Morphol. 84, 233–253.

McGann, C.J., Odelberg, S.J., Keating, M.T., 2001. Mammalian myotube dedifferentiation induced by newt regeneration extract. Proc. Natl. Acad. Sci. U. S. A. 98, 13699–13704.

Mescher, A.L., 1982. Neurotrophic control of events in injured forelimbs of larval urodeles. J. Embryol. Exp. Morphol. 69, 183–192.

Mir, L.M., Bureau, M.F., Gehl, J., Rangara, R., Rouy, D., Caillaud, J.M., Delaere, P., Branellec, D., Schwartz, B., Scherman, D., 1999. High-efficiency gene transfer into skeletal muscle mediated by electric pulses. Proc. Natl. Acad. Sci. U. S. A. 96, 4262–4267.

Odelberg, S.J., Kollhoff, A., Keating, M.T., 2000. Dedifferentiation of mammalian myotubes induced by msx1. Cell 103, 1099–1109.

Onda, H., Goldhamer, D.J., Tassava, R.A., 1990. An extracellular matrix molecule of newt and axolotl regenerating limb blastemas and embryonic limb buds: immunological relationship of MT1 antigen with tenascin. Development 108, 657–668.

Onda, H., L., P.M., Tassava, R.A., Chiu, I.M., 1991. Characterization of a newt tenascin cDNA and localization of tenascin mRNA during newt limb regeneration by in situ hybridization. Dev. Biol. 148, 219–232.

O'Steen, W.K., 1958. Regeneration of the intestine in adult urodeles. J. Morphol. 103, 435–477.

Peadon, A.M., Singer, M., 1966. The blood vessels of the regenerating limb of the adult newt, Triturus. J. Morphol. 118, 79–89.

Rageh, M.A., Mendenhall, L., Moussad, E.E., Abbey, S.E., Mescher, A.L., Tassava, R.A., 2002. Vasculature in pre-blastema and nerve-dependent blastema stages of regenerating forelimbs of the adult newt, *Notophthalmus viridescens*. J. Exp. Zool. 292, 255–266.

Reynolds, S., Holder, N., Fernandes, M., 1983. The form and structure of supernumerary hindlimbs formed following skin grafting and nerve deviation in the newt *Triturus cristatus*. J. Embryol. Exp. Morphol. 77, 221–241.

Schnapp, E., Tanaka, E.M., 2005. Quantitative evaluation of morpholino-mediated protein knockdown of GFP, MSX1, and PAX7 during tail regeneration in *Ambystoma mexicanum*. Dev. Dyn. 232, 162–170.

Semenza, G.L., Jiang, B.H., Leung, S.W., Passantino, R., Concordet, J.P., Maire, P., Giallongo, A., 1996. Hypoxia response elements in the aldolase A, enolase 1, and lactate dehydrogenase A gene promoters contain essential binding sites for hypoxia-inducible factor 1. J. Biol. Chem. 271, 32529–32537.

Smith, A.R., Wolpert, L., 1975. Nerves and angiogenesis in amphibian limb regeneration. Nature 257, 224–225.

Sukharev, S.I., Klenchin, V.A., Serov, S.M., Chernomordik, L.V., Chizmadzhev Yu, A., 1992. Electroporation and electrophoretic DNA transfer into cells. The effect of DNA interaction with electropores. Biophys. J. 63, 1320–1327.

Thornton, C.S., 1938a. The histogenesis of muscle in the regenerating fore limb of larval amblystoma punctatum. J. Morphol. 62, 17–47.

Thornton, C.S., 1938b. The histogenesis of the regenerating forelimb of larval Amblystoma after exarticulation of the humerus. J. Morphol. 62, 219–235.

Tsonis, P.A., 1996. Limb Regeneration. Cambridge Univ. Press, New York.

Tsonis, P.A., Eguchi, G., 1981. Carcinogens on regeneration. Effects of *N*-methyl-*N*′-nitro-*N*-nitrosoguanidine and 4-nitroquinoline-1-oxide on limb regeneration in adult newts. Differentiation 20, 52–60.

Turner, J.E., Singer, M., 1974a. An electron microscopic study of the newt (*Triturus viridescens*) optic nerve. J. Comp. Neurol. 156, 1–18.

Turner, J.E., Singer, M., 1974b. The ultrastructure of regeneration in the severed newt optic nerve. J. Exp. Zool. 190, 249–268.

Vinarsky, V., Atkinson, D.L., Stevenson, T.J., Keating, M.T., Odelberg, S.J.,

2005. Normal newt limb regeneration requires matrix metalloproteinase function. Dev. Biol. 279, 86–98.
Wallace, H., 1981. Vertebrate Limb Regeneration. John Wiley and Sons, New York.
Yuen, T., Wurmbach, E., Pfeffer, R.L., Ebersole, B.J., Sealfon, S.C., 2002. Accuracy and calibration of commercial oligonucleotide and custom cDNA microarrays. Nucleic Acids Res. 30, e48.
Zhou, T., Braunhut, S.J., Medeiros, D., Marx, K.A., 1998. Potential dependent endothelial cell adhesion, growth and cytoskeletal rearrangement. Material Research Society Journal 489, 211–216.